

# 2D Unitary ESPRIT for Efficient 2D Parameter Estimation

Martin Haardt,<sup>1</sup> Michael D. Zoltowski,<sup>2</sup> Cherian P. Mathews,<sup>3</sup> and Josef A. Nossek<sup>1</sup>

1. Inst. of Network Theory & Circuit Design  
Technical University of Munich  
D-80290 Munich, Germany

2. School of Electrical Engineering  
Purdue University  
West Lafayette, IN 47907-1285, U.S.A.

3. Dept. of Electrical & Computer Engin.  
Rose-Hulman Inst. of Technology  
Terre Haute, IN 47803-3999, U.S.A.

**Abstract** — Consider multiple narrowband signals that are incident upon a planar sensor array. *2D Unitary ESPRIT* is a new closed-form high resolution algorithm to provide automatically paired source azimuth and elevation angle estimates, along with an efficient way to reconstruct the impinging signals. In the final stage of the algorithm, the real and imaginary parts of the  $i$ th eigenvalue of a matrix are one-to-one related to the respective direction cosines of the  $i$ th source relative to the two array axes. *2D Unitary ESPRIT* offers several advantages over other recently proposed *ESPRIT* based closed-form 2D angle estimation techniques. First, except for the final eigenvalue decomposition of dimension equal to the number of sources, it is efficiently formulated in terms of real-valued computation throughout. Second, it is amenable to an efficient DFT beamspace implementation. Third, it is also applicable to array configurations that do not exhibit three identical subarrays, as long as the array is centro-symmetric and possesses invariances in two distinct directions, cf. Fig. 2. Finally, *2D Unitary ESPRIT* easily handles sources having one member of the spatial frequency coordinate pair in common.

## 1. Introduction

The extension of *ESPRIT*-like high resolution signal parameter estimation schemes to the 2D case, like the estimation of azimuth and elevation angles, has generally been considered a nontrivial task. This is due to the fact that, after decomposing the 2D problem into two independent 1D problems, the resulting two decoupled parameter sets have to be combined to correct parameter pairs [14, 6]. Recently proposed solutions like *Multiple Invariance ESPRIT* [8, 7] and Clark & Scharf's *2D IQML* algorithm [1] involve nonlinear optimization. In the Algebraically Coupled Matrix Pencil (*ACMP*) method of van der Veen *et al.* [9],<sup>1</sup> eigenvector information is employed to pair the respective members of the two sets of 1D angle estimates. However, under the assumption that the array lies in the  $x$ - $y$  plane, *ACMP* breaks down if two sources have the same arrival angle relative to either the  $x$ -axis or the  $y$ -axis. In contrast, for a uniform circular array (UCA) the recently presented *UCA-ESPRIT* [5] algorithm provides closed-form, automatically paired 2D angle estimates as long as the azimuth and elevation angle of each signal arrival is unique. Here, we develop a closed-form 2D angle estimation algorithm for 2D centro-symmetric array configurations, such as uniform rectangular arrays (URAs), that provide automatic pairing in a similar fashion. In the derivation of *UCA-ESPRIT* it was necessary to approximate the sampled aperture

pattern by the continuous aperture pattern. Such an approximation is not required in the development of *2D Unitary ESPRIT*. Another advantage is that *2D Unitary ESPRIT* can also be applied to array configurations that do not exhibit three identical subarrays, e.g., two noncollinear uniform linear arrays. *ACMP*, however, requires an array of sensor triplets so that one can extract three identical subarrays from the overall array. *2D Unitary ESPRIT* only requires that the array has invariances in two distinct directions.

*Unitary ESPRIT* retains the simplicity and high-resolution capability of the original *ESPRIT* algorithm for one-dimensional (1D) arrays, but attains a superior performance for correlated signals at a reduced computational cost. Being completely formulated in terms of real-valued computations, *1D Unitary ESPRIT* represents a simple and efficient method to constrain the estimated phase factors to the unit circle [3]. Since the dimension of the matrices is not increased, this completely real-valued algorithm achieves a substantial reduction of the computational complexity. Both, the element space version [3] and the DFT beamspace version [13] of *1D Unitary ESPRIT* formulate each of the three primary stages of the algorithm in terms of real-valued computations: (1) the computation of the signal eigenvectors, (2) the solution to the overdetermined system of equations derived from these signal eigenvectors, and (3) the computation of the eigenvalues of the solution to the system of equations formed in stage 2. The ability to formulate *ESPRIT*-like algorithms for 1D array structures that only require real-valued computations from start to finish, after an initial sparse unitary (or beamspace) transformation, is critically important in developing *2D Unitary ESPRIT*.

## 2. 2D Array Geometry

Consider a two-dimensional (2D) centro-symmetric sensor array of  $M$  elements lying in the  $x$ - $y$  plane (Fig. 1). A sensor array is called centro-symmetric [11], if its element locations are symmetric with respect to the centroid and the complex responses of paired elements are the same. Assume that the array also exhibits a dual invariance, i.e., two identical subarrays of  $m_x$  elements are displaced by  $\Delta_x$  along the  $x$ -axis, and another pair of identical subarrays, consisting of  $m_y$  elements each, is displaced by  $\Delta_y$  along the  $y$ -axis. Notice that the four subarrays can overlap and  $m_x$  is not required to equal  $m_y$ . Such array configurations include uniform rectangular arrays (URAs), uniform rectangular frame arrays (URFAs), i.e., URAs without some of their center elements, and cross arrays consisting of two orthogonal linear arrays with a common phase center, cf. Fig. 2.<sup>2</sup>

This work was supported by the German Research Foundation (DFG) under contract no. 322-730, by the National Science Foundation under grant no. MIP-9320890, and by AFOSR under contract no. F49620-92-J-0198 in conjunction with Wright Laboratories.

<sup>1</sup>van der Veen *et al.* do not actually give their method a name. In a later paper [10] Vanpoucke *et al.* label their method *ACMP*.

<sup>2</sup>In the examples of Fig. 2, all values of  $m_x$  and  $m_y$  correspond to selection matrices with maximum overlap in both directions. For a URA of  $M = M_x \times M_y$  elements, cf. Fig. 2 (a), this assumption implies  $m_x = (M_x - 1) M_y$  and  $m_y = M_x (M_y - 1)$ .

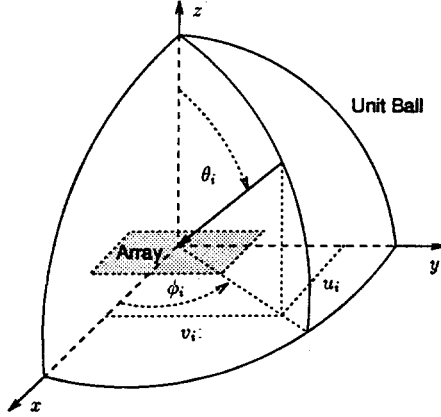


Fig. 1: Definitions of azimuth ( $-180^\circ < \phi_i \leq 180^\circ$ ) and elevation ( $0^\circ \leq \theta_i \leq 90^\circ$ )

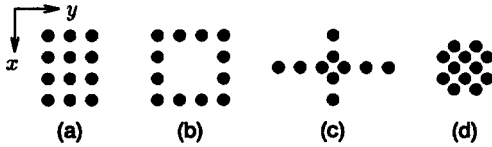


Fig. 2: Centro-symmetric array configurations with a dual invariance structure: (a) URA with  $M = 12, m_x = 9, m_y = 8$ . (b) URFA with  $M = 12, m_x = m_y = 6$ . (c) Cross array with  $M = 10, m_x = 3, m_y = 5$ . (d)  $M = 12, m_x = m_y = 7$ .

Incident on the array are  $d$  narrow-band planar wavefronts with wavelength  $\lambda$ , azimuth  $\phi_i$  and elevation  $\theta_i$ ,  $1 \leq i \leq d$ . Let  $u_i = \cos \phi_i \sin \theta_i$  and  $v_i = \sin \phi_i \sin \theta_i$  denote the direction cosines of the  $i$ th source relative to the  $x$ - and  $y$ -axes, respectively (Fig. 1). The  $d$  impinging signals are combined to a column vector  $s(t)$ . Furthermore,  $n(t)$  denotes the additive noise vector, which is assumed to be spatially white and uncorrelated with the signals. Then, the array measurements are given by  $x(t) = As(t) + n(t) \in \mathbb{C}^M$ , where the sensor outputs at time  $t$  are stacked in a column vector  $x(t)$ , such that the array steering matrix  $A \in \mathbb{C}^{M \times d}$  satisfies  $\Pi_M A = A\Lambda$  for some unitary diagonal matrix  $\Lambda \in \mathbb{C}^{d \times d}$ .  $\Pi_M$  is the  $M \times M$  exchange matrix with ones on its antidiagonal and zeros elsewhere. Throughout this paper, an overbar denotes complex conjugation without transposition. Every row of the array steering matrix  $A$  corresponds to an element of the sensor array.

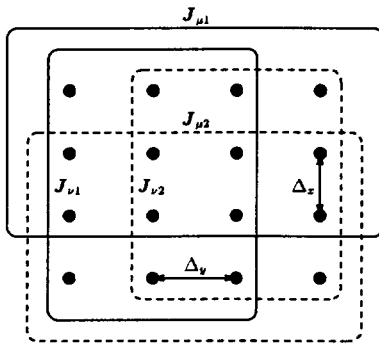


Fig. 3: Subarray selection for a URA of  $M = 4 \times 4 = 16$  sensor elements (maximum overlap in both directions:  $m_x = m_y = 12$ )

Thus, we can define two pairs of selection matrices that are centro-symmetric with respect to one another, i.e.,

$$J_{\mu 2} = \Pi_{m_x} J_{\mu 1} \Pi_M \quad \text{and} \quad J_{\nu 2} = \Pi_{m_y} J_{\nu 1} \Pi_M. \quad (1)$$

Fig. 3 visualizes a possible choice of the selection matrices for a URA of  $M = 4 \times 4 = 16$  sensor elements. Then, the steering matrix  $A$  satisfies the following invariance properties

$$J_{\mu 1} A \Phi_\mu = J_{\mu 2} A \quad \text{with} \quad \Phi_\mu = \text{diag} \{ e^{j\mu_i} \}_{i=1}^d \quad (2)$$

$$J_{\nu 1} A \Phi_\nu = J_{\nu 2} A \quad \text{with} \quad \Phi_\nu = \text{diag} \{ e^{j\nu_i} \}_{i=1}^d. \quad (3)$$

where  $\mu_i = \frac{2\pi}{\lambda} \Delta_x u_i$  and  $\nu_i = \frac{2\pi}{\lambda} \Delta_y v_i$  are the spatial frequencies in  $x$ - and  $y$ -direction, respectively. The data matrix  $X$  will be an  $M \times N$  matrix composed of  $N$  snapshots  $x(t_n)$ ,  $1 \leq n \leq N$ , of data as columns.

### 3. 2D Unitary ESPRIT in Element Space

In the 1D case, *Unitary ESPRIT* retains an *ESPRIT*-like structure, except for the fact that it is formulated in terms of real-valued computations from start to finish [3]. The real-valued implementation was derived by exploiting a bijective mapping between centro-Hermitian and real matrices [4]. A complex-valued matrix  $M \in \mathbb{C}^{p \times q}$  is called *centro-Hermitian* if  $\Pi_p \bar{M} \Pi_q = M$ . Furthermore, define left  $\Pi$ -real matrices [4, 3] as matrices  $Q \in \mathbb{C}^{p \times q}$  satisfying  $\Pi_p Q = Q$ . The unitary matrix

$$Q_{2n+1} = \frac{1}{\sqrt{2}} \begin{bmatrix} I_n & 0 & jI_n \\ 0^T & \sqrt{2} & 0^T \\ \Pi_n & 0 & -j\Pi_n \end{bmatrix}, \quad (4)$$

for example, is left  $\Pi$ -real of odd order. A unitary left  $\Pi$ -real matrix of size  $2n \times 2n$  is obtained from (4) by dropping its center row and center column. More left  $\Pi$ -real matrices can be constructed by post-multiplying a left  $\Pi$ -real matrix  $Q$  by an arbitrary real matrix  $R$ , i.e., every matrix  $QR$  is left  $\Pi$ -real. The real implementation of *Unitary ESPRIT* is based on the following theorem.

**Theorem 1 ([4])** Let  $Q_p$  and  $Q_q$  denote unitary, left  $\Pi$ -real matrices of size  $p \times p$  and  $q \times q$ , respectively. Then, the bijective mapping

$$\varphi : M \mapsto Q_p^H M Q_q$$

maps the set of all  $p \times q$  centro-Hermitian matrices onto  $\mathbb{R}^{p \times q}$ , the set of all real matrices of the same size.

As in the 1D case, an SVD of the complex-valued “extended” data matrix  $\begin{bmatrix} X & \Pi_M \bar{X} \Pi_N \end{bmatrix}$  corresponds to a square-root version of the familiar forward-backward averaging scheme. Notice that this “extended” data matrix is *centro-Hermitian*. Thus, it can be transformed into a real-valued matrix of the same size by using theorem 1,

$$T(X) \triangleq Q_M^H \begin{bmatrix} X & \Pi_M \bar{X} \Pi_N \end{bmatrix} Q_{2N} \in \mathbb{R}^{M \times 2N}. \quad (5)$$

If  $Q$  denotes the left  $\Pi$ -real matrix defined in (4), an efficient computation of the transformation  $T(X) \in \mathbb{R}^{M \times 2N}$  from the complex-valued data matrix  $X$  only requires  $M \times 2N$  real additions [3]. Its  $d$  dominant left singular vectors  $E_s \in \mathbb{R}^{M \times d}$  are obtained through a real-valued SVD of  $T(X)$  (direct data or square-root approach). Alternatively, they can be computed through a real-valued eigen-decomposition of  $T(X)T(X)^H \in \mathbb{R}^{M \times M}$  (covariance approach).

To invert the transformation in (5), define  $C_{\mu k} = J_{\mu k} Q_M E_s \in \mathbb{C}^{m_x \times d}$  for  $k = 1, 2$ . Then, it is well known that an estimate of the phase factors  $e^{j\mu_i}$ ,  $1 \leq i \leq d$ , is given by the eigenvalues of  $\Psi_\mu$ , where  $\Psi_\mu$  is a solution of the overdetermined complex-valued set of equations

$$C_{\mu 1} \Psi_\mu \approx C_{\mu 2}. \quad (6)$$

However, it was shown in [3] that an estimate of the spatial frequencies in  $x$ -direction,  $\mu_i$ ,  $1 \leq i \leq d$ , can more efficiently be obtained from the solution of the overdetermined real-valued set of equations

$$K_{\mu 1} E_s \Upsilon_\mu \approx K_{\mu 2} E_s, \quad (7)$$

where the selection matrices  $K_{\mu 1}$  and  $K_{\mu 2}$  are obtained from  $J_{\mu 1}$  and  $J_{\mu 2}$  in the following fashion:

$$\begin{aligned} K_{\mu 1} &= Q_{m_x}^H (J_{\mu 1} + J_{\mu 2}) Q_M \\ K_{\mu 2} &= Q_{m_x}^H j (J_{\mu 1} - J_{\mu 2}) Q_M \end{aligned}$$

Since the matrices in braces are centro-Hermitian,  $K_{\mu 1}$  and  $K_{\mu 2}$  are real-valued according to theorem 1. They are even sparse, if the selection matrix  $J_{\mu 1}$  is sparse. Notice that the real-valued system of equations (7) has the same dimension, i.e.,  $m_x \times d$ , as its complex-valued counterpart (6). Moreover, the total least squares (TLS) solution of the complex-valued system (6)  $\Psi_\mu^{(TL)}$  and the TLS solution of the real-valued system (7)  $\Upsilon_\mu^{(TL)}$  are related via the linear fractional transformation

$$f(x) = -\frac{x-j}{x+j}, \quad (8)$$

which is analytic for  $x \neq -j$ , namely  $\Psi_\mu^{(TL)} = f(\Upsilon_\mu^{(TL)})$ . To achieve additional computational savings, the TLS solution of (7)  $\Upsilon_\mu^{(TL)}$  can be replaced by its least squares (LS) solution, which is a simplification of the algorithm that does not affect the accuracy of the resulting estimates [3].

Let  $\Upsilon_\mu = T \Omega_\mu T^{-1}$  be an eigendecomposition of the real matrix  $\Upsilon_\mu$ , i.e., the LS or TLS solution of (7). Then, the eigenvalues of  $\Psi_\mu$  can be obtained through the same linear fractional transformation, that is

$$\Phi_\mu = f(\Omega_\mu) \quad \text{with} \quad \Omega_\mu = \text{diag}\{\omega_{\mu_i}\}_{i=1}^d \quad (9)$$

and  $\omega_{\mu_i} \neq -j$ . Furthermore, the associated eigenvectors of  $\Upsilon_\mu$  and  $\Psi_\mu$  are the same. Notice also that solving (9) for  $\omega_{\mu_i}$  yields

$$\omega_{\mu_i} = \frac{1}{j} \frac{e^{j\mu_i} - 1}{e^{j\mu_i} + 1} = \tan\left(\frac{\mu_i}{2}\right). \quad (10)$$

This reveals a spatial frequency warping identical to the temporal frequency warping incurred in designing a digital filter from an analog filter via the bilinear transformation.

The spatial frequencies in  $y$ -direction,  $\nu_i$ ,  $1 \leq i \leq d$ , are estimated in a similar fashion. First, define the real-valued selection matrices

$$\begin{aligned} K_{\nu 1} &= Q_{m_y}^H (J_{\nu 1} + J_{\nu 2}) Q_M \\ K_{\nu 2} &= Q_{m_y}^H j (J_{\nu 1} - J_{\nu 2}) Q_M. \end{aligned}$$

Then,  $\Phi_\nu = f(\Omega_\nu)$  is determined from the eigendecomposition of the (T)LS solution of the overdetermined real-valued system of equations

$$K_{\nu 1} E_s \Upsilon_\nu \approx K_{\nu 2} E_s. \quad (11)$$

Assuming a large number of snapshots  $N$ , the following asymptotic observations are made. They are critical to achieve automatic pairing of the diagonal elements of  $\Phi_\mu$  and  $\Phi_\nu$ . First, the  $d \times d$  matrix of eigenvectors  $T$  in the spectral decomposition of  $\Upsilon_\mu = T \Omega_\mu T^{-1}$  is the same as that appearing in the spectral decomposition of  $\Upsilon_\nu = T \Omega_\nu T^{-1}$ . Second, we can choose a real-valued eigenvector matrix  $T$ . The subspace spanned by the columns of  $T$  is unique as long as no two sources have exactly the same azimuth and elevation angles. Finally,  $\Upsilon_\mu$  and  $\Upsilon_\nu$  are real-valued, as are the diagonal matrices  $\Omega_\mu$  and  $\Omega_\nu$ . Automatic pairing of the spatial frequency estimates  $\mu_i$  and  $\nu_i$  is achieved by computing the eigendecomposition of the "complexified" matrix

$$\Upsilon_\mu + j \Upsilon_\nu = T (\Omega_\mu + j \Omega_\nu) T^{-1}, \quad (12)$$

where the real and the imaginary part of the eigenvalues is asymptotically given by

$$\Omega_\mu = \text{diag}\{\tan(\mu_i/2)\}_{i=1}^d \quad \text{and} \quad \Omega_\nu = \text{diag}\{\tan(\nu_i/2)\}_{i=1}^d.$$

Notice that *2D Unitary ESPRIT* is symmetric with respect to the  $x$ - and  $y$ -axes, whereas many other methods, like *ACMP* or *2D IQLM*, do not treat the estimation of  $u_i$  and  $v_i$  alike. The maximum number of sources *2D Unitary ESPRIT* can handle is  $\min\{m_x, m_y\}$ , assuming that at least  $d+1$  snapshots are available. If only a single snapshot is available (or more than two sources are correlated), one can extract  $d+1$  or more identical subarrays out of the overall array to get the effect of multiple snapshots (spatial smoothing), thereby decreasing the maximum number of sources that can be handled.

Reconstructing the impinging wavefronts (signal copy) only requires a few additional computations. Asymptotically the array steering matrix  $A$  and  $Q_M E_s$  span the same column space. Thus, there exists a full rank matrix  $\tilde{T} \in \mathbb{C}^{d \times d}$  such that

$$A = Q_M E_s \tilde{T}. \quad (13)$$

It turns out that  $\tilde{T} = T D^{-1}$ , where  $T$  is the matrix of eigenvectors obtained from (12) and  $D \in \mathbb{C}^{d \times d}$  denotes some diagonal scaling matrix. Using (13) as an estimate of  $A$ , a linear estimate of the source signal matrix  $S \in \mathbb{C}^{d \times N}$  takes the form [2]

$$\hat{S} = (A^H A)^{-1} A^H X = (D T^{-1} E_s^H Q_M^H) X. \quad (14)$$

Each row of  $\hat{S}$  contains a signal vector corresponding to one source. A brief summary of the whole algorithm is given in table 1.

#### 4. 2D Unitary ESPRIT in DFT Beamspace

Reduced dimension processing in DFT beamspace is facilitated when one has a-priori information on the general angular locations of the signal arrivals, as in a radar application, for example. In this case, we can restrict the computations to those rows of the DFT matrix that form beams encompassing the sector of interest, thereby yielding reduced computational complexity. If there is no a-priori information, one may examine the DFT spectrum and apply *2D Unitary ESPRIT* in DFT beamspace to a small set of DFT values around each spectral peak above a particular threshold. In a more general setting, *2D Unitary ESPRIT* in DFT beamspace can simply be applied via parallel processing to each of a number of sets of successive DFT values corresponding to overlapping sectors.

Similar to *Unitary ESPRIT* in element space [3], and in contrast to the *Beamspace ESPRIT* algorithm of Xu *et al.* [12], the

Table 1: Summary of 2D Unitary ESPRIT in element space

1. *Signal Subspace Estimation*: Compute  $\mathbf{E}_s \in \mathbb{R}^{M \times d}$  as the  $d$  dominant left singular vectors of  $\mathbf{T}(\tilde{\mathbf{X}}) \in \mathbb{R}^{M \times 2N}$  (square-root approach) or the  $d$  dominant eigenvectors of  $\mathbf{T}(\tilde{\mathbf{X}})\mathbf{T}(\tilde{\mathbf{X}})^H \in \mathbb{R}^{M \times M}$  (covariance approach).

2. *(Total) Least Squares*: Then, solve

$$\underbrace{\mathbf{K}_{\mu 1} \mathbf{E}_s}_{\mathbb{R}^{m_x \times d}} \underbrace{\mathbf{\Upsilon}_\mu}_{\mathbb{R}^{m_x \times d}} \approx \underbrace{\mathbf{K}_{\mu 2} \mathbf{E}_s}_{\mathbb{R}^{m_x \times d}} \quad \text{and} \quad \underbrace{\mathbf{K}_{\nu 1} \mathbf{E}_s}_{\mathbb{R}^{m_y \times d}} \underbrace{\mathbf{\Upsilon}_\nu}_{\mathbb{R}^{m_y \times d}} \approx \underbrace{\mathbf{K}_{\nu 2} \mathbf{E}_s}_{\mathbb{R}^{m_y \times d}}$$

by means of (total) least squares techniques.

3. *Spatial Frequency Estimation*: Calculate the eigendecomposition of the complex-valued  $d \times d$  matrix

$$\mathbf{\Upsilon}_\mu + j \mathbf{\Upsilon}_\nu = \mathbf{T} \mathbf{\Lambda} \mathbf{T}^{-1} \quad \text{with} \quad \mathbf{\Lambda} = \text{diag} \{ \lambda_i \}_{i=1}^d$$

- $\mu_i = 2 \arctan(\text{Re} \{ \lambda_i \}) \quad i = 1, 2, \dots, d$
- $\nu_i = 2 \arctan(\text{Im} \{ \lambda_i \}) \quad i = 1, 2, \dots, d$

4. *Signal Reconstruction*: Estimate  $\hat{\mathbf{S}}$  according to (14).

DFT beamspace version of 1D Unitary ESPRIT involves only real-valued computation from start to finish after the initial transformation to beamspace. Again, this is critically important for an extension to the 2D case, since after decomposing the 2D problem into two independent (real-valued) 1D problems, the resulting two parameter sets are combined to correct parameter pairs through a complex-valued eigendecomposition similar to equation (12). Details can be found in [13].

## 5. Simulations

The presented simulations compare the performance of 2D Unitary ESPRIT in element space with that of ACMP and the Cramér-Rao (CR) lower bound [5], using a URA of  $M = 5 \times 5 = 25$  elements,  $N = 40$  snapshots, and 500 trial runs. Three uncorrelated, equi-powered sources are located at  $(u_1, v_1) = (0.5, 0.2)$ ,  $(u_2, v_2) = (0.4, 0.3)$ , and  $(u_3, v_3) = (0.3, 0.4)$ . Fig. 4 depicts the the RMSE (in the  $u$ - $v$  plane) as a function of the SNR, while Fig. 5 shows scatter plots of the DOA estimates for an SNR of 10 dB. Compared to ACMP, 2D Unitary ESPRIT achieves a significantly better performance with a reduced computational complexity.

## 6. Concluding Remarks

2D Unitary ESPRIT is a new closed-form ESPRIT-like high resolution algorithm to provide automatically paired 2D spatial frequency estimates in element space or DFT beamspace. Except for the final eigendecomposition of dimension  $d$ , it is efficiently formulated in terms of real-valued computation throughout. Since the impinging wavefronts can easily be reconstructed, 2D Unitary ESPRIT is particularly attractive for spatial diversity reception with antenna arrays to improve the performance of mobile communication systems. Moreover, 2D Unitary ESPRIT can also be employed in a variety of applications other than array signal processing, including 2D harmonic retrieval for image analysis and high resolution radar imaging.

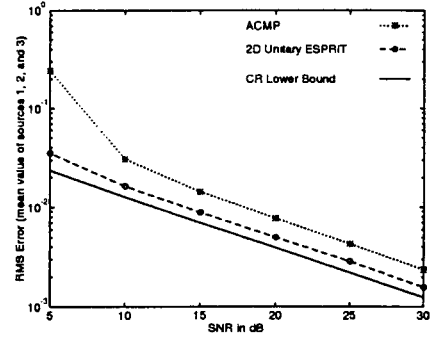


Fig. 4: Mean value of the RMS error for the 3 sources in the  $u$ - $v$  plane as a function of the SNR.

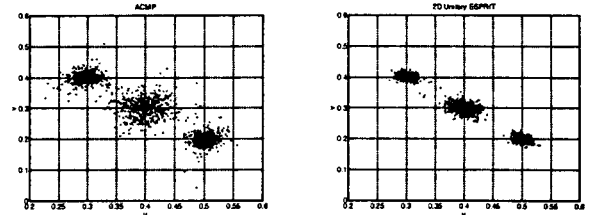


Fig. 5: Scatter plots of the DOA estimates in the  $u$ - $v$  plane for ACMP (left) and 2D Unitary ESPRIT (right), SNR = 10 dB.

## References

- [1] M. P. Clark and L. L. Scharf, "Two-dimensional modal analysis based on maximum likelihood", *IEEE Trans. Signal Processing*, vol. 42, pp. 1443–1452, June 1994.
- [2] M. Haardt and M. E. Ali-Hackl, "Unitary ESPRIT: How to exploit additional information inherent in the rotational invariance structure", in *Proc. IEEE Int. Conf. Acoust., Speech, Signal Processing*, vol. IV, pp. 229–232, Adelaide, Australia, Apr. 1994.
- [3] M. Haardt and J. A. Nossek, "Unitary ESPRIT: How to obtain increased estimation accuracy with a reduced computational burden", *IEEE Trans. Signal Processing*, vol. 43, May 1995, scheduled to appear.
- [4] A. Lee, "Centrohermitian and skew-centrohermitian matrices", *Linear Algebra and its Applications*, vol. 29, pp. 205–210, 1980.
- [5] C. P. Mathews and M. D. Zoltowski, "Eigenstructure techniques for 2-D angle estimation with uniform circular arrays", *IEEE Trans. Signal Processing*, vol. 42, pp. 2395–2407, Sept. 1994.
- [6] M. P. Pepin and M. P. Clark, "On the performance of several 2-D harmonic retrieval techniques", in *Proc. 28th Asilomar Conference on Signals, Systems, and Computers*, Pacific Grove, CA, Nov. 1994, to be published.
- [7] A. L. Swindlehurst and T. Kailath, "Azimuth/elevation direction finding using regular array geometries", *IEEE Trans. Aerospace and Electronic Systems*, vol. 29, pp. 145–156, Jan. 1993.
- [8] A. L. Swindlehurst, B. Ottersten, R. Roy, and T. Kailath, "Multiple invariance ESPRIT", *IEEE Trans. Signal Processing*, vol. 40, pp. 867–881, Apr. 1992.
- [9] A. J. van der Veen, P. B. Ober, and E. F. Deprettere, "Azimuth and elevation computation in high resolution DOA estimation", *IEEE Trans. Signal Processing*, vol. 40, pp. 1828–1832, July 1992.
- [10] F. Vanpoucke, M. Moonen, and Y. Berthoumieu, "An efficient subspace algorithm for 2-D harmonic retrieval", in *Proc. IEEE Int. Conf. Acoust., Speech, Signal Processing*, vol. IV, pp. 461–464, Adelaide, Australia, Apr. 1994.
- [11] G. Xu, R. H. Roy, and T. Kailath, "Detection of number of sources via exploitation of centro-symmetry property", *IEEE Trans. Signal Processing*, vol. 42, pp. 102–112, Jan. 1994.
- [12] G. Xu, S. D. Silverstein, B. Ottersten, M. Viberg, and T. Kailath, "Beamspace ESPRIT", *IEEE Trans. Signal Processing*, vol. 42, pp. 349–356, Feb. 1994.
- [13] M. D. Zoltowski, M. Haardt, and C. P. Mathews, "Closed-form 2D angle estimation with rectangular arrays via DFT beamspace ESPRIT", in *Proc. 28th Asilomar Conference on Signals, Systems, and Computers*, Pacific Grove, CA, Nov. 1994, to be published.
- [14] M. D. Zoltowski and D. Stavrinos, "Sensor array signal processing via a Procrustes rotations based eigenanalysis of the ESPRIT data pencil", *IEEE Trans. Acoust., Speech, Signal Processing*, vol. ASSP-37, pp. 832–861, June 1989.